Experimental Observation on Enhancement of the Ambipolar Potential by Injection of Neutral Beams in a Tandem Mirror

K. Yatsu, S. Miyoshi, H. Tamai, K. Shida, K. Ishii, and A. Itakura
Institute of Physics, The University of Tsukuba, Sakura-Mura, Ibaraki 300-31, Japan
(Received 4 April 1979)

Neutral hydrogen beams of 13 and 14 keV at equivalent proton currents of 5 and 3 A, respectively, were injected into a target plasma in a tandem mirror. The space potential at plugs increased more than 10 V relative to the space potential at the central cell and was sustained for more than 0.3 ms. The potential increase is due to the heating of electrons with trapped hot ions and is explained by the relation $\varphi = T_e \ln(n_p/n_c)$.

The tandem mirror concept[1,2] have been introduced as a means to increase the plasma confinement time in open systems. Many theoretical studies[3,4] have been reported in connection with the tandem mirror concept. Several tandem mirror devices have been designed or constructed and some of them have started experimental studies very recently. The production of the confining potential by injection of neutral beams has been experimentally verified by Miyoshi *et al.*[5] We report here experimental observations on enhancement and sustainment of the ambipolar potential by injection of neutral beams in the tandem mirror.

A schematic setup of the tandem mirror device (GAMMA6) is shown in Fig. 1. Two minimum-B magnetic wells (plugs) are produced by two regular Yin-Yang pairs[6] with major radius of 40 cm and minor radius of 13 cm. They are connected by a nearly uniform solenoid (central cell). The mirror ratio of the minimum-B magnetic well is 1:2.3. Two solenoidal coils are placed at outsides of the Yin-Yang pairs to produce guide field, respectively. The magnetic flux tubes in the plugs entering the solenoid are oriented to face one another. The GAMMA6 has no recircularizing coil so that a circular magnetic flux tube with a diameter of 6 cm at the plug center elongates into an elliptical cross section of 2.4 cm × 42 cm at center of the central cell. The magnetic field strength at the plug center is 4 kG and that in the central cell is 1.5 kG. The distance between centers of two plugs is 315 cm. The internal diameter of the vacuum chamber of the central cell is 42 cm. The vacuum chamber is evacuated to less than 5×10^{-7} Torr. Titanium films are deposited on walls of injector tanks, beam-dump tanks, and plug chambers.

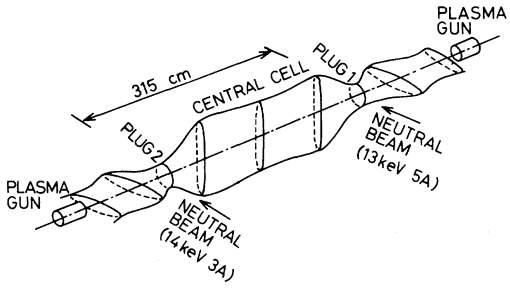

FIG. 1. Schematic setup of the GAMMA6.

The hydrogen target plasma produced by Ti-washer plasma guns at both ends lasts for about 0.45 ms. Neutral hydrogen beams are injected by a Lawrence Berkeley Laboratory (LBL)-10A-type and a LBL-30A-type source.[7] The pulse length of the beams is 2.5 ms. The plasma guns are fired at a time 0.5 ms after the initiation of neutral-beam injection. Diagnostics consist of double probes, an 8-mm microwave interferometer, and a neutral-particle energy analyzer.

The plasma density of the target plasma was typically 1.5×10^{13} cm^{-3} in the plugs and $(0.2\text{–}1.0) \times 10^{13}$ cm^{-3} in the central cell. The floating potential V_f on the axis was about −20 V in the plugs

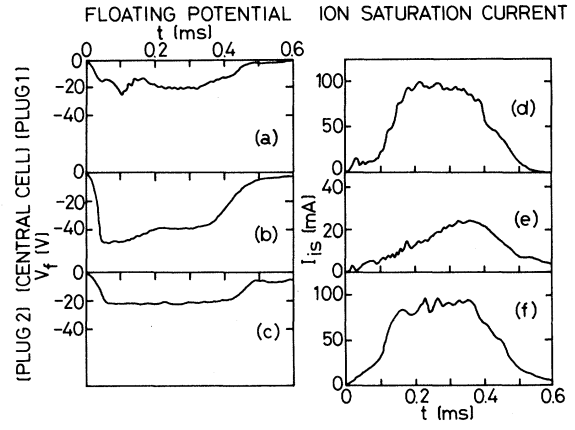

FIG. 2. Wave forms of the floating potential (a), (c) in plugs and (b) in central cell, and the ion saturation current (d), (f) in plugs and (e) in central cell. The ion saturation current of 100 mA corresponds to the plasma density of 1.7×10^{13} cm^{-3}.

and −40 V in the central cell, where the reference of the potential was the earth potential. The value and time behavior of the floating potential and those of the plasma density were almost the same in both plugs when characteristics of the plasma guns were carefully adjusted. Typical wave forms of the floating potential and ion saturation current I_{is} in the three portions are shown in Fig. 2. Large fluctuations were not observed in the target plasma. The time behavior of the electron temperature T_e is shown in Fig. 3, where subscript 0 indicates the case without beam.

Since the main interest is the potential difference between the plug and central cell, signals of the floating potential at the plug V_{fp0}, and that at the central cell V_{fc0} were fed to a differential amplifier and the difference signal $V_{fp0} - V_{fc0}$ was recorded for eight to ten shots, where subscripts p and c indicate the plug and central cell, respectively. The averaged value is shown in Fig. 4. The graph corresponds to the time behavior of the difference of space potential between the plug and central cell because the electron temperature was nearly equal in the two portions. The difference of the space potential φ_0 is expressed by

$$\varphi_0 = T_{e0} \ln(n_{p0}/n_{c0}) . \quad (1)$$

The potential difference is calculated for the time behavior of the plasma density shown in Fig. 2, and that of the electron temperature shown in Fig. 3, and is shown in Fig. 4. The difference of the space potential of the target plasma behaves as expected by the relation (1).

Neutral beams of 3.1×10^{19} H^0/sec (equivalent to 5A H^+) at 13 keV and 1.9×10^{19} H^0/sec (equivalent to 3A H^+) at 14 keV were injected into the plug 1 and plug 2, respectively. The electron temperature increased about 6 eV in both plugs, but the increase was less than 4 eV in the central cell as shown in Fig. 3. There was a little difference in plasma behavior in the plug 1 and plug 2 because of the difference in injected beams. However, the plasma behavior was essentially the same in both plugs, so that our discussions will be concentrated on relations between the plug 1 and central cell.

The measurement of trapped hot ions was carried out to see the relation between the electron temperature and hot-ion density. The hot ions were observed with the neutral-particle energy analyzer, however, the hot-ion density n_h was not determinable. Then, n_h is estimated by a buildup calculation. Assuming a constant target plasma density n_t, the hot-ion density buildup

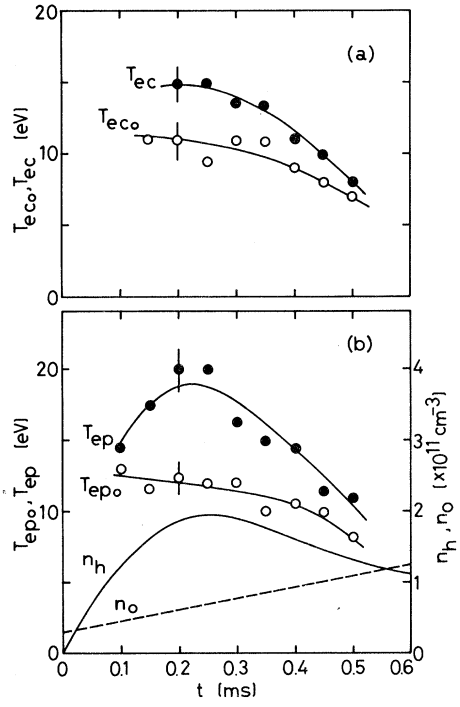

FIG. 3. Time behavior of the electron temperature T_{ec0}, T_{ec} in the central cell and T_{epo}, T_{ep} in the plug, and the calculated hot-ion density n_n. The neutral gas density n_0 is estimated from measurements of the gas pressure for independent operation of the beams alone and the plasma guns alone.

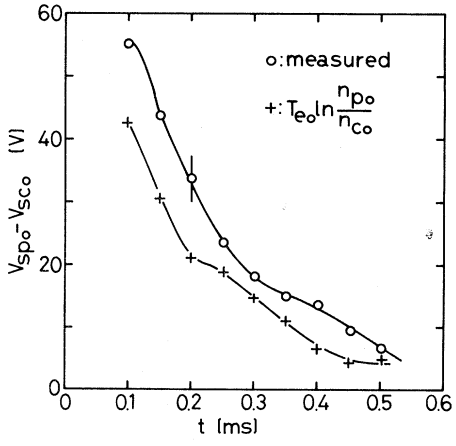

FIG. 4. Time behavior of the difference of the space potential between the plug and central cell for the case without beam. Circles, measured; pluses, calculated with use of T_{e0}, n_{p0}, and n_{c0}.

rate is[8]

$$\frac{1}{n_h+n_t}\frac{dn_h}{dt}=\frac{2R_pI}{eV_p}(\sigma_i+\alpha\sigma_x)-\frac{1-\alpha}{\tau}. \quad (2)$$

Here, R_p and V_p are the plasma radius and volume, I is the equivalent current of the neutral beam, σ_i and σ_x are ionization and charge exchange cross sections, τ is the loss time of hot-ion, and α is the fraction of the target plasma $\alpha = n_t/(n_h+n_t)$. The loss time of hot ions is mainly determined by the charge-exchange reactions. The neutral gas originates from the charge-exchange reactions of the neutral beam with the target plasma. In the present case, however, much more gas was produced by a fraction of the injected neutral beam, which struck the chamber wall since the half-angle of divergence of the beam was about 2°. The pumping speed was not enough to evacuate the gas thus produced. The increase of the pressure was measured by a nude ion gauge to be 2×10^{-3} Torr/s. The increase of the pressure due to the target plasma was also measured under a condition of the magnetic field strength of 200 G since the nude ion gauge did not work under the experimental condition of 4 kG. The pressure increase due to the target plasma was estimated to be the same amount with that due to the neutral beam. The hot-ion density is calculated by the relation (2) taking into account the gas load which is shown by a dotted line in Fig. 3(b). As shown in Fig. 3(b), the hot-ion density increases at first but it decreases again because the charge-exchange loss-time decreases due to the increase in gas pressure. The increase in the electron temperature is explainable by heating of the electrons with trapped hot ions and taking into account the energy transfer time from hot ions to electrons and the energy balance.

By injection of the beams, the floating potential at the plug increased by several volts, but the increase was smaller at the central cell. In order to measure the effect of the beam injection on the floating potential, the difference voltage $V_{fp}-V_{fc}$ was recorded for eight to ten shots for the case with neutral beams. The averaged values were compared for the two cases with neutral beams and without beam. Figure 5 shows the increase in the difference of the floating potential, $V_f-V_{f0}=(V_{fp}-V_{fc})-(V_{fp0}-V_{fc0})$ by injection of the beams. The floating potential and space potential are related by $V_s=V_f+3.1T_e$ for hydrogen plasma.[9] In the present case, the magnetic field was so strong that electrons were magnetized. Ions, however, were unmagnetized, for the

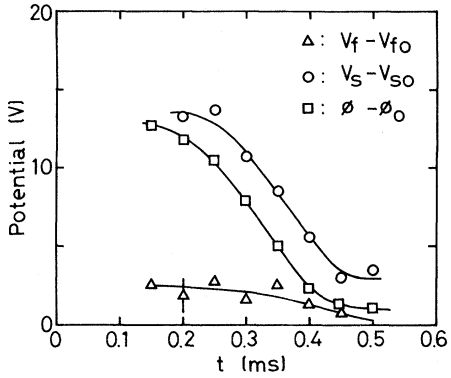

FIG. 5. Time behavior of the potential differences V_f-V_{f0}, V_s-V_{s0}, and $\varphi-\varphi_0$ between the cases with beams and without a beam.

Larmor radius of ions was much larger than the probe radius. Then, the increase in the difference of the space potential by beam injection is expressed by

$$V_s-V_{s0}=V_f-V_{f0}+3.1[(T_{ep}-T_{ec})-T_{ep0}-T_{ec0})]. \quad (3)$$

The time behavior of V_s-V_{s0} is shown in Fig. 5. In the case of beam injection, the electron temperature differs a little between the plug and central cell. However, the potential difference between the two portions may be approximated by Eq. (1) because the difference in electron temperature is small compared with the electron temperature. The increase of the potential difference by the increase in electron temperature is approximated by $\varphi-\varphi_0=T_{ep}\ln(n_p/n_c)-T_{ep0}\ln(n_{p0}/n_{c0})$, where T_{ep} is used as the heated-electron temperature. The potential increase thus calculated roughly agrees with the measured value V_s-V_{s0} (Fig. 5).

In summary, the potential difference between the plugs and central cell increased more than 10 V by injection of neutral beams. The potential increase was sustained for more than 0.3 ms, which was mainly limited by the duration of the target plasma but was much longer than the time to arrive at a steady-state condition in so far as the electrons were concerned. The potential increase is due to the heating of electrons with trapped hot ions and is explained by Eq. (1).

[1]G. I. Dimov, V. V. Zakaidakov, and M. E. Kishinevski, Fiz. Plazmy 2, 597 (1976) [Sov. J. Plasma Phys.

2, 326 (1976)].
[2]T. K. Fowler and B. G. Logan, Comments Plasma Phys. Cont. Fusion 2, 167 (1977).
[3]D. E. Baldwin *et al.*, in *Proceedings of the Seventh International Conference on Plasma Physics and Controlled Nuclear Fusion Research, Innsbruck, Austria, 1978* (International Atomic Energy Agency, Vienna, Austria, 1979), paper No. CN-37-J-4.
[4]B. G. Logan *et al.*, Ref. 3, paper No. CN-37-R-3.
[5]S. Miyoshi *et al.*, Ref. 3, paper No. CN-37-J-5.
[6]R. W. Moir and R. F. Post, Nucl. Fusion 9, 253 (1969).
[7]W. R. Baker *et al.*, in *Proceedings of the Fifth International Conference on Plasma Physics and Controlled-Nuclear Fusion Research, Tokyo, Japan, 1974* (International Atomic Energy Agency, Vienna, Austria, 1975), paper No. CN-33-D2-2.
[8]F. H. Coensgen, W. F. Cummins, B. G. Logan, A. W. Molvik, W. E. Nexsen, T. C. Simonen, B. W. Stallard, and W. C. Turner, Phys. Rev. Lett. 35, 1501 (1975).
[9]F. F. Chen, in *Plasma Diagnostic Techniques*, edited by R. H. Huddlestone and S. L. Leonard (Academic, New York, 1965), p. 113.

Structure of the Smectic-*B* Phase and the Nature of the Smectic-*B* to -*H* Transition in the N-(4-*n*-Alkoxybenzylidene)-4′-Alkylanilines

A. J. Leadbetter, M. A. Mazid, and B. A. Kelly
Chemistry Department, University of Exeter, Exeter EX4 4QD, England

and

J. W. Goodby and G. W. Gray
Chemistry Department, University of Hull, Hull HU6 7RX, England
(Received 30 January 1979)

The phase behavior and structures of several liquid crystals of the *n*O.*m* (C_nH_{2n+1}-OPhCHNPhC_mH_{2m+1}) series of compounds have been established by a variety of experiments. The hexagonal close-packed layers of the S_B phases have a bilayer stacking sequence. The structure is increasingly modulated with decreasing temperature by periodic displacements of the molecules along their long axes. An additional displacement of this type occurs at the S_B-S_H transition.

Many physical studies have been made of the liquid-crystal phases of the N-(4-*n*-alkoxybenzylidene)-4′-alkylanilines, for although these compounds have simple chemical structures they exhibit complex smectic polymorphism.[1,2] These compounds have the general structure of Fig. 1 and because of the use of *n* and *m* to denote the length of the terminal alkyl chains, they are often known as the *n*O.*m*'s.

We have prepared a variety of these compounds in order to study the different types of smectic phase sequence which they exhibit. The transition temperatures and phase sequences for a number of these compounds are summarized in Table I, in which the code letters designating the different phases are those recommended previously.[3] The phase sequences shown for these materials

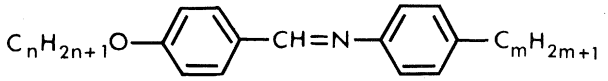

FIG. 1. Structure of the *n*O.*m* compounds.

have been confirmed by optical microscopy, miscibility studies, differential-scanning calorimetry, and x-ray analysis, the details of which will be published elsewhere.

Certain of the materials studied, e.g., 5O.7 and 7O.5, exhibit well-defined smectic-*B* and smectic-*H* phases which confirms the existence of S_B-S_H transitions and gives separate identities to each phase. An extremely detailed investigation of the smectic-*B* phases exhibited by these materials was carried out and the microscopic textures of the S_B phases of a number of these compounds were found to be slightly abnormal. These materials were therefore examined carefully by x-ray diffraction to establish whether this microscopic feature had any structural significance. The first results of this investigation are described here since they have led to quite new results concerning the structure of the S_B phases and the nature of the $S_B \rightleftharpoons S_H$ transitions.

The x-ray measurements were mostly made on aligned samples, in ~ 1-mm Lindemann glass tubes, prepared by slow cooling from the nemat-